Structure of molten lanthanum and cerium tri-halides by the method of isomorphic substitution in neutron diffraction

1999 J. Phys.: Condens. Matter 11 1381

(http://iopscience.iop.org/0953-8984/11/6/004)

J. Phys.: Condens. Matter **11** (1999) 1381–1396. Printed in the UK PII: S0953-8984(99)98445-X

Structure of molten lanthanum and cerium tri-halides by the method of isomorphic substitution in neutron diffraction

Jonathan C Wasse† and Philip S Salmon‡

School of Physics, University of East Anglia, Norwich NR4 7TJ, UK

Received 16 October 1998

Abstract. The total structure factors of the molten trivalent metal halides MX_3, where M^{3+} denotes La^{3+} or Ce^{3+} and X^- denotes Cl^-, Br^- or I^-, have been measured by using neutron diffraction. Difference function methods were then applied on assuming that the LaX_3 and CeX_3 melts for a given halide ion are isomorphic. The results which follow from this assumption show that the first sharp diffraction peak in the measured total structure factors arises from cation correlations and its movement to lower scattering vector values with increasing anion size is consistent with an enhanced separation in real space of cation centred polyhedra. On melting the MX_3 salts exhibit a decrease in the coordination number of both the cations and anions. In the liquid state the M–X coordination environment is asymmetric with M–Cl, M–Br and M–I nearest-neighbour distances of 2.93(2) Å, 3.01(2) Å, 3.18(2) Å and M–Cl, M–Br and M–I coordination numbers of 8.2(2), 7.4(2), 6.7(2) respectively. The Cl–Cl, Br–Br and I–I nearest-neighbour distances are 3.58(3) Å, 3.76(3) Å, 4.13(2) Å respectively and there is a significant penetration of the X–X partial pair distribution function into the first peak of the M–X partial pair distribution function for all three anions. The Cl–Cl, Br–Br and I–I coordination numbers are 9.2(2), 8.7(2) and 8.2(2) respectively if the M–M coordination number is two.

1. Introduction

The object of this paper is to present neutron diffraction results on the structure of the molten trivalent metal halides MX_3 where M^{3+} denotes La^{3+} or Ce^{3+} and X^- denotes Cl^-, Br^- or I^-. Specifically, if the LaX_3 and CeX_3 melts for a given halide ion can be regarded as isomorphic then since the cation coherent neutron scattering lengths are significantly different (Sears 1992) it is possible to simplify the complexity of correlations associated with a single neutron diffraction measurement by the application of difference function methods (see e.g. Salmon *et al* 1998). Isomorphism is expected on the basis that lanthanum and cerium have similar physical and chemical properties (Cotton and Wilkinson 1988), the ionic radii of La^{3+} and Ce^{3+} are comparable (Shannon 1976) and corresponding LaX_3 and CeX_3 systems crystallize in the same structure as expected from the similar Pettifor (1986) chemical parameters of $\chi_{La} = 0.705$ and $\chi_{Ce} = 0.7025$. Furthermore, LaX_3 and CeX_3 for a given anion melt with a similar entropy change ΔS_m (Dworkin and Bredig 1971, see also Gaune-Escard *et al* 1994) and the ionic conductivity, κ_m, of the liquids at the melting point, T_m, is comparable (see table 1).

† Now at: Department of Physics and Astronomy, University College London, Gower Street, London WC1E 6BT, UK.

‡ Author for correspondence. Now at: Department of Physics, University of Bath, Bath BA2 7AY, UK.

0953-8984/99/061381+16$19.50

Table 1. The room temperature crystal structure type (Wells 1984), melting point T_m (Dworkin and Bredig 1971), entropy change on melting ΔS_m (Dworkin and Bredig 1971), ionic conductivity at the melting point κ_m and volume change $\Delta V/V_m$ (see text) for LaX_3 and CeX_3.

	$LaCl_3$	$CeCl_3$	$LaBr_3$	$CeBr_3$	LaI_3	CeI_3
Crystal structure	UCl_3	UCl_3	UCl_3	UCl_3	$PuBr_3$	$PuBr_3$
T_m (°C)	858	817	788	732	778	760
ΔS_m (cal K^{-1} mol^{-1})	11.5	11.7	12.3	12.4	12.7	12.0
κ_m (Ω^{-1} cm^{-1})	1.2–1.5[a,b]	0.8–1.1[b]	0.6–0.8[c]		0.4[d,e]	0.4[d]
$\Delta V/V_m$ (%)	16	18	12		24	

[a] Janz *et al* (1975), Fukushima *et al* (1991).
[b] Gaune *et al* (1996).
[c] Yaffe and van Artsdalen (1956), Fukushima and Iwadate (1996).
[d] Janz *et al* (1968).
[e] Janz *et al* (1977).

Motivation for the study of these molten MX_3 systems is provided by the absence of a systematic study on the effect of the anion size on the liquid structure. As the anion radius increases from 1.81 Å for Cl^- to 2.20 Å for I^- via 1.96 Å for Br^- (Shannon 1976) the anion polarizability increases and the $PuBr_3$-type structure is stabilized over the UCl_3-type structure in the solid state (Wells 1984). It is therefore interesting to find the concomitant change in the liquid structure, especially as recent computer simulation studies, using an ionic interaction model that includes an account of ionic polarization phenomena, indicate that the basic microscopic properties of MX_3 materials might be understood in terms of the interplay between polarization effects and ion size (Madden and Wilson 1996). Experimental results will enable the potentials used in these computer simulation studies to be tested.

2. Theory

In a neutron diffraction experiment on a molten MX_3 salt comprising rare-earth paramagnetic cations the differential scattering cross section per ion for unpolarized neutrons can be written as

$$\left(\frac{d\sigma}{d\Omega}\right)_{tot} = \left(\frac{d\sigma}{d\Omega}\right)_{mag} + \left(\frac{d\sigma}{d\Omega}\right)_{nucl}. \tag{1}$$

In the free ion approximation there is no applied magnetic field, the effect of the 'crystalline' electric field on the cation can be neglected and the cation ground state is given by Russell–Saunders (L–S) coupling and Hund's rules. The paramagnetic differential scattering cross section is then given by (Balcar and Lovesey 1989)

$$\left(\frac{d\sigma}{d\Omega}\right)_{mag} = c_M(\gamma r_e)^2 \frac{1}{6} J(J+1) g_J^2 \mathcal{F}^2(k) \tag{2}$$

where c_M is the atomic fraction of the cation, $\gamma = 1.913$ is the magnitude of the neutron magnetic moment in units of the nuclear magneton, r_e is the classical radius of an electron such that $(\gamma r_e)^2 = 0.2906$ barn, J is the total angular momentum quantum number and g_J is the Landé splitting factor (Bleaney and Bleaney 1989). The magnetic form factor, $\mathcal{F}(k)$, is obtained from the expression

$$\mathcal{F}^2(k) = \langle j_0(k)\rangle^2 + C_{02}\langle j_0(k)\rangle\langle j_2(k)\rangle + C_{22}\langle j_2(k)\rangle^2 + C_{24}\langle j_2(k)\rangle\langle j_4(k)\rangle + C_{44}\langle j_4(k)\rangle^2 + C_{46}\langle j_4(k)\rangle\langle j_6(k)\rangle + C_{66}\langle j_6(k)\rangle^2 \tag{3}$$

where k is the magnitude of the scattering vector, the radial integrals $\langle j_K(k)\rangle$ for $K = 0$, 2, 4 and 6 are given by Freeman and Desclaux (1979) (see also Brown 1995), the coefficients C_{ij} ($i = 0$, 2, 4 or 6, $j = 2$, 4 or 6), are given in appendix E.3 of Balcar and Lovesey (1989) and in the limit as $k \to 0$, $\mathcal{F}(0) = 1$. The 'dipole approximation' (Johnston 1966) in which terms in $\langle j_K(k)\rangle$ for $K > 2$ are neglected was not applied as neutrons of relatively high energy were used in the diffraction experiments. The nuclear differential scattering cross section is given by

$$\left(\frac{\mathrm{d}\sigma}{\mathrm{d}\Omega}\right)_{nucl} = F(k) + \sum_{\alpha} c_\alpha[b_\alpha^2 + b_{inc,\alpha}^2][1 + P_\alpha(k)] \tag{4}$$

where the total structure factor is defined by

$$F(k) = c_M^2 b_M^2[S_{MM}(k) - 1] + 2c_M c_X b_M b_X[S_{MX}(k) - 1] + c_X^2 b_X^2[S_{XX}(k) - 1] \tag{5}$$

$S_{\alpha\beta}(k)$ is a Faber–Ziman partial structure factor, c_α, b_α, $b_{inc,\alpha}$ denote the atomic fraction, coherent scattering length and incoherent scattering length of chemical species α and $P_\alpha(k)$ is the inelasticity correction for chemical species α (Howe *et al* 1989).

If diffraction experiments are made on molten LaX_3 and on molten CeX_3 for fixed X^- under comparable conditions and if the melts can be regarded as isomorphic following the discussion in section 1, then subtraction of the resultant total structure factors, $F_{La}(k)$ and $F_{Ce}(k)$, gives the first order difference function

$$\begin{aligned}\Delta_M(k) \equiv F_{La}(k) - F_{Ce}(k) &= c_M^2(b_{La}^2 - b_{Ce}^2)[S_{MM}(k) - 1] \\ &+2c_M c_X(b_{La} - b_{Ce})b_X[S_{MX}(k) - 1]\end{aligned} \tag{6}$$

which contains only the cation correlations. The complexity of correlations associated with the total structure factors can also be reduced by forming the difference function

$$\begin{aligned}\Delta F'(k) &= F_{La}(k) - b_{La}\Delta_M(k)/(b_{La} - b_{Ce}) = F_{Ce}(k) - b_{Ce}\Delta_M(k)/(b_{La} - b_{Ce}) \\ &= -c_M^2 b_{La} b_{Ce}[S_{MM}(k) - 1] + c_X^2 b_X^2[S_{XX}(k) - 1]\end{aligned} \tag{7}$$

in which the M–X correlations are eliminated. The values of the weighting coefficients in equations (5)–(7), calculated using $b_{La} = 8.24(4)$ fm, $b_{Ce} = 4.84(2)$ fm, $b_{Cl} = 9.5770(8)$ fm, $b_{Br} = 6.795(15)$ fm and $b_I = 5.28(2)$ fm (Sears 1992), are given in table 2. The scattering lengths give the cation correlations a larger relative weighting with increasing anion size.

Table 2. The weighting coefficients on the $S_{\alpha\beta}(k)$ contributing to the total structure factor $F(k)$ and the difference functions $\Delta_M(k)$ and $\Delta F'(k)$ for molten LaX_3 and CeX_3 salts.

Salt or isomorphic pair	$c_M^2 b_M^2$ (mbarn)	$2c_M c_X b_M b_X$ (mbarn)	$c_X^2 b_X^2$ (mbarn)	$-c_M^2 b_{La} b_{Ce}$ (mbarn)	$c_M^2(b_{La}^2 - b_{Ce}^2)$ (mbarn)	$2c_M c_X(b_{La} - b_{Ce})b_X$ (mbarn)
$LaCl_3$	42.4(4)	296(1)	515.9(1)	—	—	—
$CeCl_3$	14.6(1)	173.8(7)	515.9(1)	—	—	—
$LaCl_3$ & $CeCl_3$	—	—	515.9(1)	−24.9(2)	27.8(4)	122(2)
$LaBr_3$	42.4(4)	210(1)	260(1)	—	—	—
$CeBr_3$	14.6(1)	123.3(6)	260(1)	—	—	—
$LaBr_3$ & $CeBr_3$	—	—	260(1)	−24.9(2)	27.8(4)	87(1)
LaI_3	42.4(4)	163(1)	157(1)	—	—	—
CeI_3	14.6(1)	95.8(5)	157(1)	—	—	—
LaI_3 & CeI_3	—	—	157(1)	−24.9(2)	27.8(4)	67(1)

The real space functions $G(r)$, $\Delta G_M(r)$ and $\Delta G'(r)$, corresponding to $F(k)$, $\Delta_M(k)$ and $\Delta F'(k)$ respectively, are obtained from equations (5)–(7) by replacing the $S_{\alpha\beta}(k)$ by the partial

pair distribution functions $g_{\alpha\beta}(r)$ whence

$$G(r) = c_M^2 b_M^2[g_{MM}(r) - 1] + 2c_M c_X b_M b_X[g_{MX}(r) - 1] + c_X^2 b_X^2[g_{XX}(r) - 1] \tag{8}$$

$$\Delta G_M(r) = c_M^2(b_{La}^2 - b_{Ce}^2)[g_{MM}(r) - 1] + 2c_M c_X(b_{La} - b_{Ce})b_X[g_{MX}(r) - 1] \tag{9}$$

and

$$\Delta G'(r) = -c_M^2 b_{La} b_{Ce}[g_{MM}(r) - 1] + c_X^2 b_X^2[g_{XX}(r) - 1]. \tag{10}$$

The mean number of particles of type β contained in a volume defined by two concentric spheres of radii r_i and r_j, centred on a particle of type α, is given by

$$\bar{n}_\alpha^\beta = 4\pi n_0 c_\beta \int_{r_i}^{r_j} r^2 g_{\alpha\beta}(r)\,\mathrm{d}r \tag{11}$$

where n_0 is the ionic number density of the melt.

Provided that the data correction procedure has been properly undertaken (Salmon and Benmore 1992, Salmon *et al* 1998) the unphysical low-r features in $G(r)$, $\Delta G_M(r)$ and $\Delta G'(r)$ should oscillate about their calculated limits of $G(0) = -(c_M b_M + c_X b_X)^2$, $\Delta G_M(0) = -\{c_M^2(b_{La}^2 - b_{Ce}^2) + 2c_M c_X(b_{La} - b_{Ce})b_X\}$ and $\Delta G'(0) = -\{c_X^2 b_X^2 - c_M^2 b_{La} b_{Ce}\}$ respectively. Further, there should be good overall agreement between the measured k-space data sets $F(k)$, $\Delta_M(k)$ and $\Delta F'(k)$ and the Fourier back-transforms $\tilde{F}(k)$, $\tilde{\Delta}_M(k)$ and $\tilde{\Delta} F'(k)$ of the corresponding r-space functions after the unphysical low-r oscillations are set to their calculated limiting values.

3. Experimental details

All of the salts, supplied by Aldrich, had a water content of less than 100 ppm and were handled either in high vacuum or under a high purity argon gas atmosphere. The $LaCl_3$ (99.99+%), $CeCl_3$ (99+%) and CeI_3 (99.999%) samples were sealed under vacuum in cylindrical silica tubes of 7 mm internal diameter and 1 mm wall thickness which had been cleaned using chromic acid followed by etching with a 25% by mass solution of hydrofluoric acid. The $LaBr_3$ (99.9%), $CeBr_3$ (99.9%) and LaI_3 (99.9%) samples were sealed under vacuum in cleaned silica tubes of 5 mm internal diameter and 1 mm wall thickness. The neutron diffraction experiments were performed using the LAD instrument at the ISIS pulsed neutron source, Rutherford Appleton Laboratory. The complete experiment comprised the measurement of the diffraction patterns for the samples in their container in a cylindrical vanadium furnace, the empty container in the furnace, the empty furnace and a vanadium rod of 8.31(4) mm diameter for normalization purposes. The data analysis was made using the ATLAS suite of programs (Soper *et al* 1989) and the nuclear cross-sections were calculated using the values of Sears (1992). The total paramagnetic scattering cross section, $\sigma_{mag}(\lambda)$, for Ce^{3+} (La^{3+} is not paramagnetic) at an incident neutron wavelength λ was obtained by integrating equation (2) over the full range of solid angle Ω. For scattering which is symmetrical about an axis defined by the incident beam

$$\sigma_{mag}(\lambda) = c_M(\gamma r_e)^2 \frac{4}{3}\pi\, J(J+1) g_J^2 \lambda^2 \int_{s=0}^{s=1/\lambda} s\mathcal{F}^2(s)\,\mathrm{d}s \tag{12}$$

where $s \equiv k/4\pi$.

LAD comprises 14 groups of detectors at scattering angles of $\pm 5^\circ$, $\pm 10^\circ$, $\pm 20^\circ$, $\pm 35^\circ$, $\pm 60^\circ$, $\pm 90^\circ$ and $\pm 150^\circ$ corresponding to instrumental resolution functions ($\Delta k/k$) of 11%, 6%, 2.8%, 1.7%, 1.2%, 0.8% and 0.5% respectively. The final $F(k)$ were constructed by merging all those diffraction patterns from the different groups that showed good agreement and it was checked that the resultant $F(k)$ tend to the correct high-k limit and obey the usual sum

rule relation (Salmon and Benmore 1992). Full details of the experiment are given by Wasse (1998) and the temperatures at which the liquids were studied are included in the following discussion on the melt densities.

A mass density of 3.17(3) g cm^{-3} for molten $LaCl_3$ at 905(3) °C was estimated from the data of Yaffe and van Artsdalen (1956) and Igarashi and Mochinaga (1987) while a mass density of 3.23(3) g cm^{-3} for molten $CeCl_3$ at 835(3) °C was obtained from the work of Mellors and Senderoff (1960), Mochinaga *et al* (1993) and Iwadate *et al* (1995). The corresponding n_0 are comparable at 0.0311(3) Å^{-3} for $LaCl_3$ and 0.0316(3) Å^{-3} for $CeCl_3$ as are the calculated volume changes $\Delta V/V_m$ of 16% for $LaCl_3$ and 18% for $CeCl_3$ where $\Delta V = V_m - V_{RT}$, V_m is the molar volume of the liquid at T_m and V_{RT} the molar volume of the salt at room temperature. The volume V_{RT} is 63.79 cm^3 mol^{-1} for $LaCl_3$ (Morosin 1968) and 62.45 cm^3 mol^{-1} for $CeCl_3$ (Kojima *et al* 1951, Templeton and Dauben 1954). Larger volume changes of 19% for $LaCl_3$ and 20% for $CeCl_3$ are calculated by using the relation between ΔS_m and $\Delta V/V_m$ given by Tallon and Robinson (1982) with parameters suitable for trivalent metal halides (Akdeniz and Tosi 1992) i.e.

$$\Delta S_m/R = 5.0 \ln 2 + 12.4 \Delta V/V_m \tag{13}$$

where R is the molar gas constant and the ΔS_m for $LaCl_3$ and $CeCl_3$ are listed in table 1.

For $LaBr_3$ at 810(3) °C a mass density of 4.45(1) g cm^{-3} was obtained from the data of Fukushima and Iwadate (1996) corresponding to $n_0 = 0.0285(3)$ Å^{-3}. These data give a volume change $\Delta V/V_m = 12\%$ which is smaller than for $LaCl_3$ even though both systems melt from the UCl_3-type structure. An even smaller $\Delta V/V_m = 3\%$ is obtained by using the densities reported by Yaffe and van Artsdalen (1956) while a larger value of 22% is calculated by using equation (13) and the ΔS_m listed in table 1. Density data for $CeBr_3$ do not appear to be available in the literature so a value of 4.52(1) g cm^{-3} at 780(3) °C was taken which corresponds to $n_0 = 0.0285(3)$ Å^{-3} and $\Delta V/V_m = 12\%$. In view of the spread of density results for $LaBr_3$ the data analysis procedure for both molten $LaBr_3$ and $CeBr_3$ was repeated using upper and lower number densities of $n_0 = 0.0316$ Å^{-3} and $n_0 = 0.0253$ Å^{-3} which correspond to $\Delta V/V_m$ of 3% and 22% respectively. The volume V_{RT} is 74.65 cm^3 mol^{-1} for $LaBr_3$ (Zachariasen 1948, Krämer *et al* 1989) and 73.27 cm^3 mol^{-1} for $CeBr_3$ (Zachariasen 1948).

For LaI_3 at 810(3) °C a mass density of 4.27(7) g cm^{-3} was obtained from the data of Kutscher and Schneider (1974) corresponding to $n_0 = 0.0198(3)$ Å^{-3}. These data give a volume change $\Delta V/V_m = 24\%$ which is the same as that calculated by using equation (13) and the ΔS_m reported in table 1. Density data for CeI_3 do not appear to be available in the literature. However, a value of 4.43(7) g cm^{-3} at 800(3) °C was calculated by using equation (13) which corresponds to $n_0 = 0.0205(3)$ Å^{-3} and $\Delta V/V_m = 21\%$. The volume V_{RT} is 92.54 cm^3 mol^{-1} for LaI_3 and 91.63 cm^3 mol^{-1} for CeI_3 (Asprey *et al* 1964).

4. Results

4.1. Molten $LaCl_3$ and $CeCl_3$

The calculated paramagnetic differential scattering cross section for Ce^{3+} used in the data analysis is shown in figure 1 together with the total structure factors for molten $LaCl_3$ at 905(3) °C and $CeCl_3$ at 835(3) °C. The $F(k)$ for liquid $LaCl_3$ is qualitatively similar to that previously measured for liquid $NdCl_3$ (Saboungi *et al* 1990), a system which also melts from the UCl_3-type structure and where the cation scattering length is comparable to that of lanthanum (Sears 1992). There is a small first sharp diffraction peak (FSDP) or pre-peak at 1.12(4) Å^{-1}

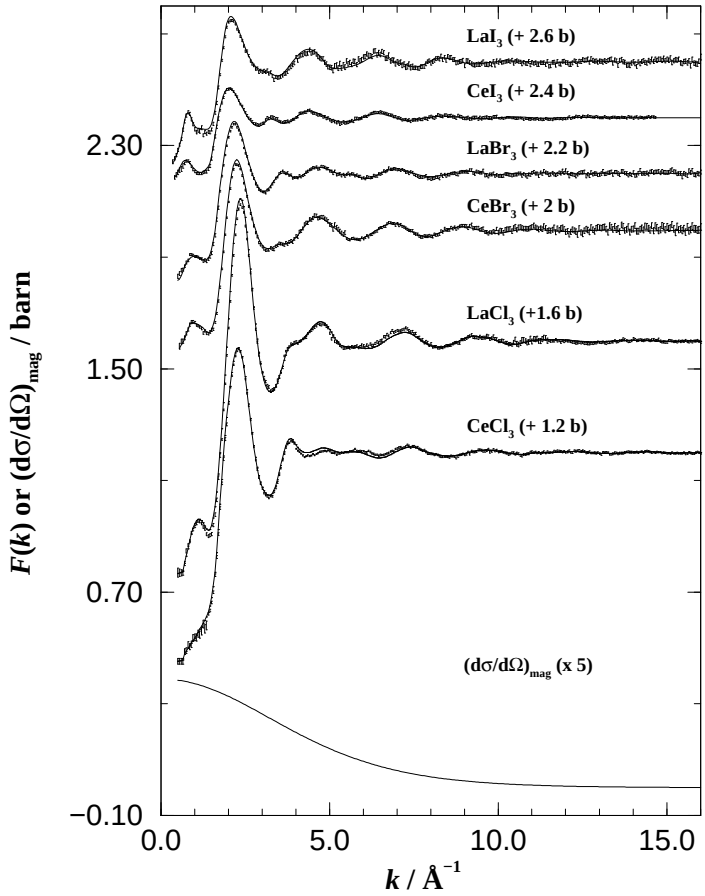

Figure 1. The measured total structure factors $F(k)$ (equation (5)) for the MX_3 molten salts (see text). The bars represent the statistical errors on the data points and the solid curves are the Fourier back-transforms of the corresponding $G(r)$ given by the solid curves in figure 2. The calculated paramagnetic differential scattering cross section $(d\sigma/d\Omega)_{mag}$ for Ce^{3+} (equation (2)) is also shown, scaled by a factor of five for clarity of presentation.

which is a signature of intermediate range ordering in the melt (see e.g. Salmon 1994). There is also a less well defined FSDP in $F(k)$ for $CeCl_3$ which reflects, in part, the use of data from a lower resolution function detector bank in the low-k region. Notwithstanding, the anion correlations have a larger relative weighting (table 2) which points to a contribution to the FSDP from the cation partial structure factors.

The corresponding $G(r)$ in figure 2 show a strong overlap between the first and second peaks occurring at 2.90(2) Å and 3.44(2) Å for $LaCl_3$ and at 2.84(2) Å and 3.51(2) Å for $CeCl_3$. It is therefore difficult to obtain reliable coordination numbers. However, if the first peak is identified with M–Cl correlations by comparison with the sum of the ionic radii for La^{3+} or Ce^{3+} and Cl^- (Shannon 1976) then its symmetrization gives $\bar{n}_M^{Cl} = 6.1(2)$ for both systems which is consistent with the $\bar{n}_{La}^{Cl}$ initially reported for molten $LaCl_3$ at 905 °C by Wasse and Salmon (1998). In x-ray diffraction total structure factor experiments on molten $LaCl_3$ at 870 °C and on molten $CeCl_3$ at 870 °C, La–Cl and Ce–Cl distances of 2.83 Å and 2.84 Å were measured together with coordination numbers of $\bar{n}_{La}^{Cl} = 5.7$ and $\bar{n}_{Ce}^{Cl} = 5.6$ (Mochinaga *et al* 1991, 1993, Iwadate *et al* 1995).

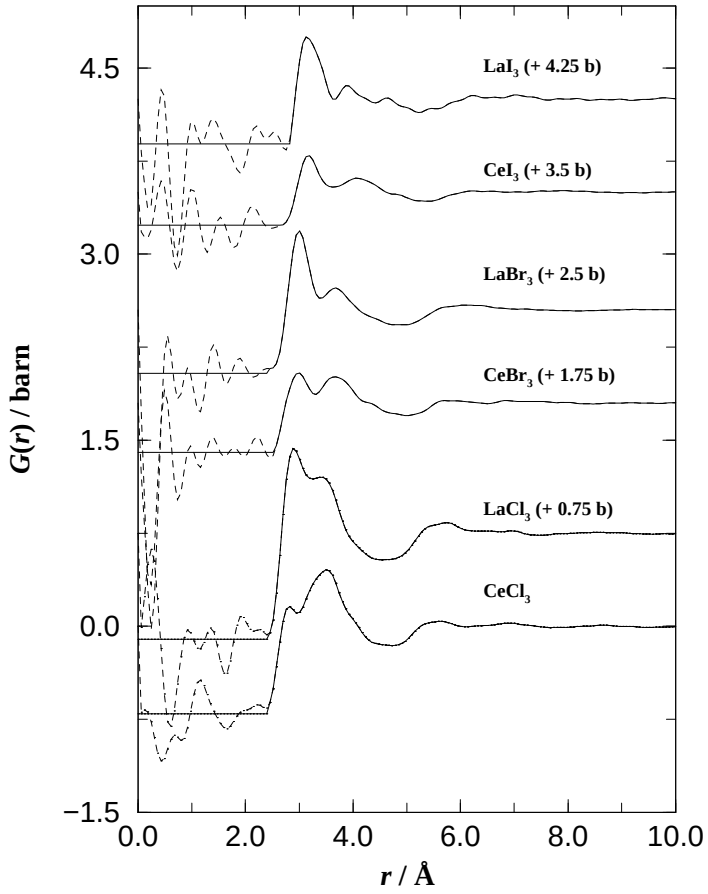

Figure 2. The total pair distribution functions $G(r)$ (equation (8)) for the MX_3 molten salts obtained by Fourier transforming the $F(k)$ given by the error bars in figure 1. The unphysical low-r oscillations about the $G(0)$ limits are shown by the broken curves.

The measured first order difference function $\Delta_M(k)$ and the corresponding $\Delta G_M(r)$ are shown in figures 3 and 4. The first peak in $\Delta G_M(r)$ at 2.93(2) Å is asymmetric and will comprise only M–Cl correlations on the basis of a comparison with the crystal structures of $LaCl_3$, in which La^{3+} is surrounded by 6 Cl^- at 2.950 Å, 3 Cl^- at 2.953 Å and 2 La^{3+} at 4.375 Å (Morosin 1968), and $CeCl_3$ (Kojima *et al* 1951). Integration of the first peak over the range $2.50(2) \leqslant r$ (Å) $\leqslant 3.37(3)$ to the first shoulder gives $\bar{n}_M^{Cl} = 6.7(2)$ while integration to the first minimum at 3.86(2) Å gives $\bar{n}_M^{Cl} = 8.2(2)$.

The difference functions $\Delta F'(k)$ and $\Delta G'(r)$ are shown in figures 5 and 6. The first peak in $\Delta G'(r)$ at 3.58(3) Å is broad and asymmetric and will comprise both Cl–Cl and M–M correlations on the basis of a comparison with the crystal structures of $LaCl_3$, in which Cl^- is surrounded by 12 Cl^- (two at 3.381 Å, four at 3.425 Å, two at 3.430 Å, two at 4.375 Å and two at 4.564 Å) and La^{3+} by 2 La^{3+} at 4.375 Å and 6 La^{3+} at 4.840 Å (Morosin 1968), and $CeCl_3$ (Kojima *et al* 1951). Integration of the first peak over the range $3.01(2) \leqslant r$ (Å) $\leqslant 4.36(3)$ to the first shoulder gives $\bar{n}_{Cl}^{Cl} = 7.4(2)$ if $\bar{n}_M^M = 0$ while integration to the first minimum at 4.79(2) Å gives $\bar{n}_{Cl}^{Cl} = 10.3(2)$ if $\bar{n}_M^M = 0$ and $\bar{n}_{Cl}^{Cl} = 9.2(2)$ if $\bar{n}_M^M = 2$.

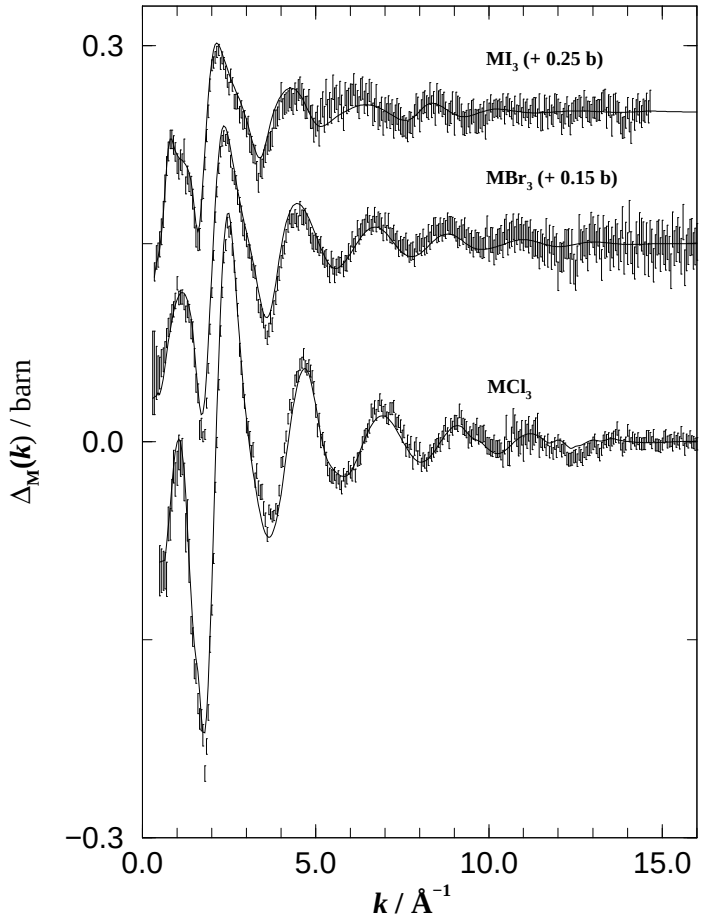

Figure 3. The measured difference functions $\Delta_M(k)$ (equation (6)) for the MCl_3, MBr_3 and MI_3 molten salts. The bars represent the statistical errors on the data points and the solid curves are the Fourier back-transforms of the corresponding $\Delta G_M(r)$ given by the solid curves in figure 4.

4.2. Molten $LaBr_3$ and $CeBr_3$

The total structure factors for molten $LaBr_3$ at 810(3) °C and $CeBr_3$ at 780(3) °C are shown in figure 1 and have FSDPs at 0.93(3) $Å^{-1}$ and 0.88(3) $Å^{-1}$ respectively. As for the chloride systems the first two peaks in the corresponding $G(r)$ at 3.00(2) Å and 3.68(2) Å for $LaBr_3$ and at 2.99(2) Å and 3.66(2) Å for $CeBr_3$ show strong overlap (see figure 2). Assignment of the first peak to M–Br correlations by comparison with the sum of the ionic radii for La^{3+} or Ce^{3+} and Br^- (Shannon 1976) gives coordination numbers of $\bar{n}^{Br}_{La} = 7.0(2)$ and $\bar{n}^{Br}_{Ce} = 7.1(2)$ by integrating over the range $2.46(2) \leqslant r$ (Å) $\leqslant 3.43(2)$ or $2.52(2) \leqslant r$ (Å) $\leqslant 3.37(2)$ respectively to the first minimum in $G(r)$.

The first order difference functions $\Delta_M(k)$ (figure 3) and $\Delta G_M(r)$ (figure 4) are qualitatively similar to those measured for the chloride melts and can be interpreted likewise since both systems melt from the UCl_3-type crystal structure wherein, for $LaBr_3$, La^{3+} is surrounded by 6 Br^- at 3.098 Å and 3 Br^- at 3.157 Å (Krämer *et al* 1989). Hence, the first asymmetric peak in $\Delta G_M(r)$ at 3.01(2) Å will comprise only M–Br correlations and its

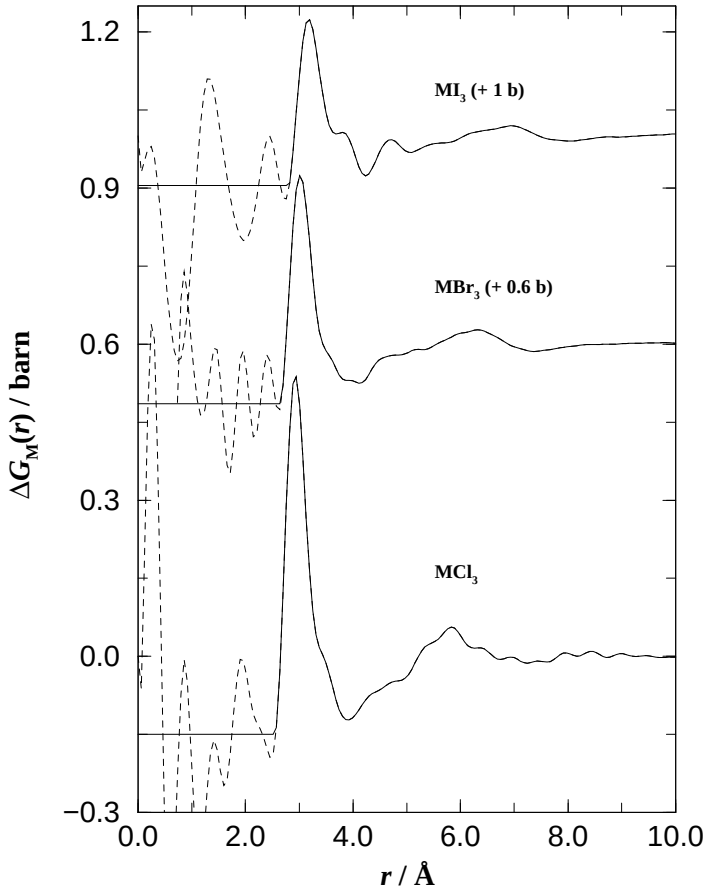

Figure 4. The real space difference functions $\Delta G_M(r)$ (equation (9)) for the MCl_3, MBr_3 and MI_3 molten salts obtained by Fourier transforming the $\Delta_M(k)$ given by the error bars in figure 3. The unphysical low-r oscillations about the $\Delta G_M(0)$ limits are shown by the broken curves.

integration over the range $2.64(2) \leqslant r$ (Å) $\leqslant 3.50(2)$ to the first shoulder gives $\bar{n}_M^{Br} = 6.1(2)$ while its integration to the first minimum at 3.72(3) Å gives $\bar{n}_M^{Br} = 7.4(2)$. The $\Delta_M(k)$ and corresponding $\Delta G_M(r)$ obtained by repeating the data analysis for the estimated upper and lower number densities had the same overall shapes and peak positions and gave coordination numbers of $\bar{n}_M^{Br} = 7.9(2)$ and $\bar{n}_M^{Br} = 6.9(2)$ respectively by integrating over the first peak in $\Delta G_M(r)$ to the same high-r value of 3.72(3) Å.

The difference functions $\Delta F'(k)$ and $\Delta G'(r)$ are shown in figures 5 and 6. As for the corresponding chloride system, the first peak in $\Delta G'(r)$ at 3.76(3) Å is broad and asymmetric and will comprise both Br–Br and M–M correlations. Integration of the first peak over the range $3.19(2) \leqslant r$ (Å) $\leqslant 4.89(3)$ to the first minimum gives $\bar{n}_{Br}^{Br} = 9.3(2)$ if $\bar{n}_M^M = 0$ and $\bar{n}_{Br}^{Br} = 8.7(2)$ if $\bar{n}_M^M = 2$, the latter corresponding to the nearest-neighbour M–M coordination number in the UCl_3-type crystal structure. The $\Delta F'(k)$ and $\Delta G'(r)$ obtained by repeating the data analysis for the estimated upper and lower number densities had the same overall shapes. A first peak position of 3.79(3) Å and coordination numbers of $\bar{n}_{Br}^{Br} = 9.8(2)$ if $\bar{n}_M^M = 0$ and $\bar{n}_{Br}^{Br} = 9.2(2)$ if $\bar{n}_M^M = 2$ were obtained for the upper number density while a first peak position of 3.70(3) Å and coordination numbers of $\bar{n}_{Br}^{Br} = 8.5(2)$ if $\bar{n}_M^M = 0$ and $\bar{n}_{Br}^{Br} = 7.9(2)$ if $\bar{n}_M^M = 2$

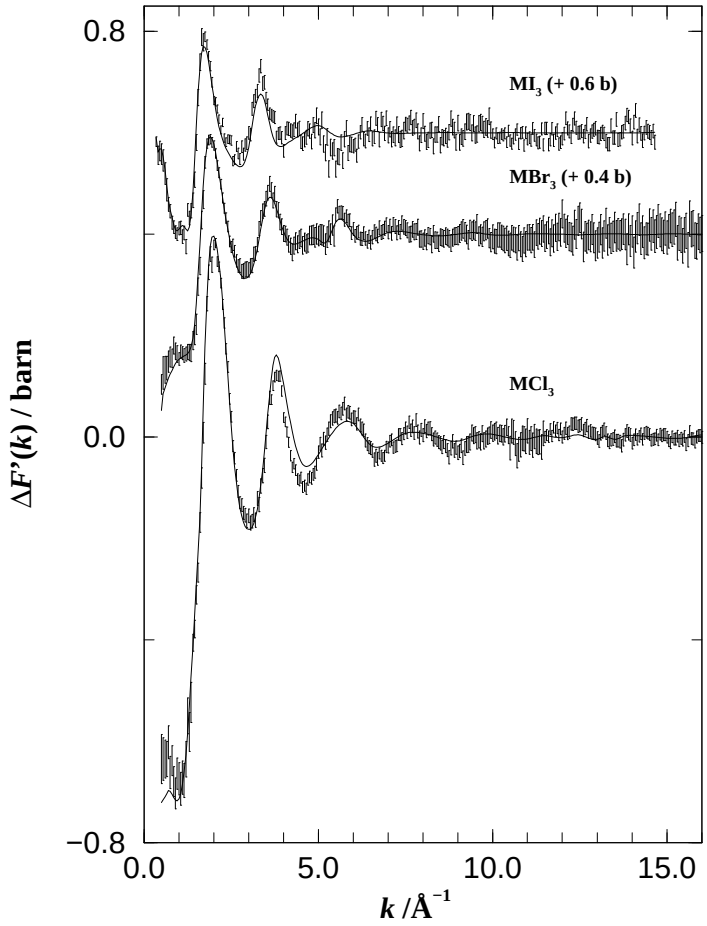

Figure 5. The measured difference functions $\Delta F'(k)$ (equation (7)) for the MCl_3, MBr_3 and MI_3 molten salts. The bars represent the statistical errors on the data points and the solid curves are the Fourier back-transforms of the corresponding $\Delta G'(r)$ given by the solid curves in figure 6.

were obtained for the lower number density where the $\bar{n}_{Br}^{Br}$ were calculated by integrating over the first peak in $\Delta G'(r)$ to the same high-r value of 4.89(3) Å.

4.3. Molten LaI_3 and CeI_3

The total structure factors for molten LaI_3 at 810(3) °C and CeI_3 at 800(3) °C are shown in figure 1 and have FSDPs at 0.81(3) $Å^{-1}$ and 0.77(3) $Å^{-1}$ respectively which occur at smaller k-values than those in the chloride and bromide systems. The first three peaks in the corresponding $G(r)$ at 3.14(2) Å, 3.96(2) Å and 4.68(2) Å for LaI_3 and at 3.17(2) Å, 4.08(2) Å and 4.89(2) Å for CeI_3 show strong overlap (see figure 2). Assignment of the first peak to M–I correlations by comparison with the sum of the ionic radii for La^{3+} or Ce^{3+} and I^- (Shannon 1976) gives coordination numbers of $\bar{n}_{La}^{I} = 6.3(2)$ and $\bar{n}_{Ce}^{I} = 6.3(2)$ by integrating over the range $2.82(2) \leqslant r$ (Å) $\leqslant 3.62(3)$ or $2.76(2) \leqslant r$ (Å) $\leqslant 3.62(3)$ respectively to the first minimum in $G(r)$.

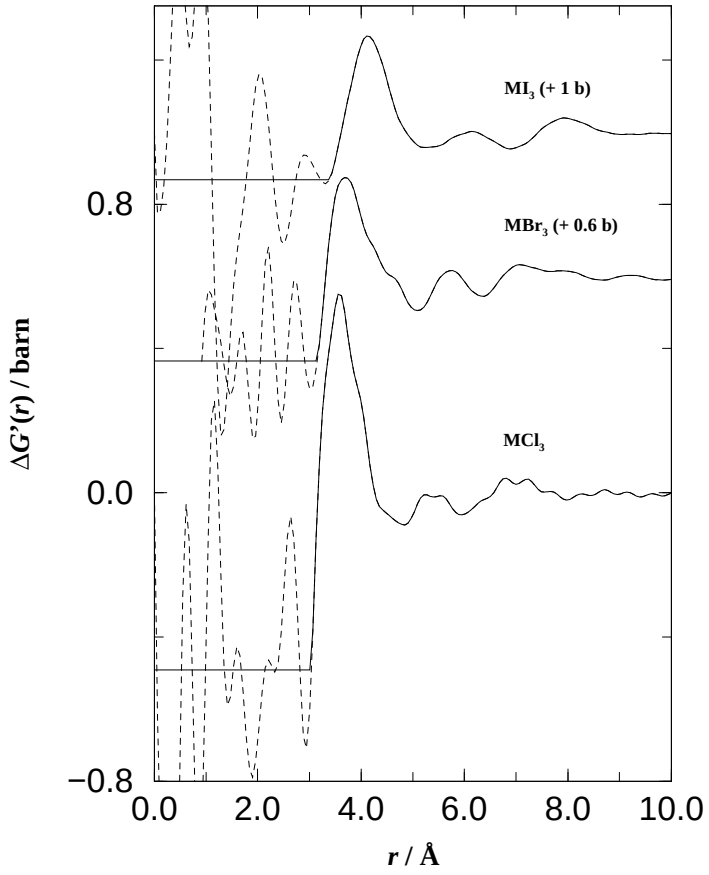

Figure 6. The real space difference functions $\Delta G'(r)$ (equation (10)) for the MCl_3, MBr_3 and MI_3 molten salts obtained by Fourier transforming the $\Delta F'(k)$ given by the error bars in figure 5. The unphysical low-r oscillations about the $\Delta G'(0)$ limits are shown by the broken curves.

The first order difference function $\Delta_M(k)$ is shown in figure 3 and the corresponding $\Delta G_M(r)$ is shown in figure 4. The first peak in $\Delta G_M(r)$ at 3.18(2) Å is assigned to M–I correlations and is asymmetric with a pronounced high-r shoulder at 3.87(2) Å. Its integration over the range $2.82(2) \leqslant r$ (Å) $\leqslant 3.62(2)$ to the start of this shoulder gives $\bar{n}_M^I = 5.1(2)$ while its integration to the first minimum at 4.23(3) Å gives $\bar{n}_M^I = 6.7(2)$. By comparison with the chloride and bromide melts, the M–M correlations have a larger weighting and the second main peak at 4.73(2) Å may therefore have a contribution from nearest-neighbour M–M correlations. This assignment together with an M–I distance of 3.18(2) Å gives an angle M–I–M of $\approx 96^\circ$ which is consistent with the M–I–M angles found in the $PuBr_3$-type crystal structure (Forrester *et al* 1964). The real space function $r^2\{\Delta G_M(r) - \Delta G_M(0)\}$ was therefore fitted by a sum of Gaussians, representing the individual partial pair-distribution functions, in the form

$$f(r) = \frac{1}{(2\pi)^{1/2}} \sum_\beta A_\beta \exp\{-(r - r_{M\beta})^2/2\sigma_\beta^2\}/\sigma_\beta \tag{14}$$

where A_β, $r_{M\beta}$ and σ_β are the area, mean position and standard deviation of Gaussian β. In this choice of fitting procedure the A_β are directly proportional to the coordination numbers

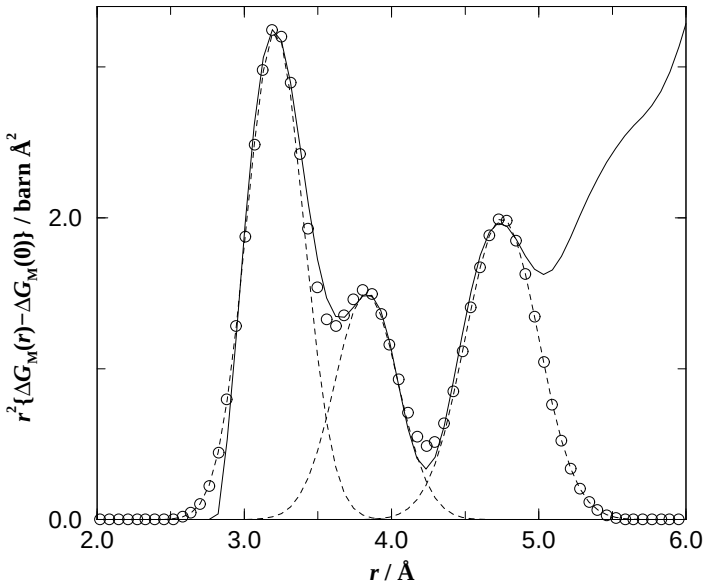

Figure 7. Fit to $r^2\{\Delta G_M(r) - \Delta G_M(0)\}$ for molten MI_3 by three Gaussians represented by the function $f(r)$ of equation (14). The solid curve gives the data, the open circles the fitted $f(r)$ and the broken curves the individual fitted Gaussians.

$\bar{n}_M^\beta$ (Lond *et al* 1991). A fit to three Gaussians is shown in figure 7 and gives coordination numbers of $\bar{n}_M^I = 4.4(3)$, $\bar{n}_M^I = 2.3(3)$ and $\bar{n}_M^M = 2.8(3)$ for the Gaussians centred at 3.25(3) Å, 3.80(3) Å and 4.70(3) Å respectively. This $\bar{n}_M^M$ compares with an M–M nearest-neighbour coordination number of two in the $PuBr_3$-type crystal structure (Forrester *et al* 1964) and presumably represents an upper limit since $g_{MI}(r)$ will also contribute to the third Gaussian region.

The difference functions $\Delta F'(k)$ and $\Delta G'(r)$ are shown in figures 5 and 6 respectively. The first peak in $\Delta G'(r)$ at 4.13(2) Å is broad, covering the range $3.37(2) \leqslant r$ (Å) $\leqslant 5.22(3)$, and by comparison with the $PuBr_3$-type crystal structure will comprise both I–I and M–M correlations. Its integration gives $\bar{n}_I^I = 9.1(2)$ if $\bar{n}_M^M = 0$ and $\bar{n}_I^I = 8.2(2)$ if $\bar{n}_M^M = 2$, the latter corresponding to the nearest-neighbour M–M coordination number in the $PuBr_3$-type crystal structure.

5. Discussion

For all of the MX_3 melts there is good overall agreement between the measured reciprocal space functions and their corresponding Fourier back-transforms which indicates that the data correction procedure has been properly undertaken (Salmon and Benmore 1992). Discrepancies do however occur for several of the functions and, although they are small when compared with the magnitude of the measured functions, they merit discussion in view of the approximations made in deriving equations (6) and (7). The discrepancies do not result from the $P_\alpha(k)$ terms in equation (4), which arise from use of the static approximation (Squires 1978), since for a given LAD detector group the $P_\alpha(k)$ correction at high-k is small and readily calculable for the relatively high atomic numbers of the chemical species present in the MX_3 melts and the data at low-k, where the correction is large, were not used to form the final $F(k)$

functions (Howe *et al* 1989). Further, the discrepancies do not result from the paramagnetic scattering correction for Ce^{3+} (equation (2)) since there are no residual slopes on the reciprocal space data sets. Instead, they are attributed to small experimental uncertainties, such as those associated with the difficulty in merging the different LAD detector groups to form the final $F(k)$ functions, rather than to a breakdown in the approximation of isomorphism. Support for this assertion is derived from the difference functions for the MBr_3 melts which were the only ones obtained from total structure factors measured consecutively for samples in the same sized containers using an identical instrument set-up during the same experimental period. Under these conditions the effect of systematic errors will be reduced (Salmon *et al* 1998) as confirmed by the good agreement at all k-values found between $\Delta_M(k)$ and $\tilde{\Delta}_M(k)$ (figure 3) and between $\Delta F'(k)$ and $\tilde{\Delta} F'(k)$ (figure 5).

Identifiable FSDPs appear in the $\Delta_M(k)$ (figure 3) for all three MX_3 systems but not in the corresponding $\Delta F'(k)$ (figure 5) which are dominated by the X–X correlations (table 2). This implies a strong contribution to the FSDPs from the cation correlations, an observation which also holds for molten divalent metal halide salts (Salmon 1992). It is also possible for a given halide ion to form a difference function between two weighted total structure factors wherein $S_{MM}(k)$ is given a zero weighting (see e.g. van der Aart *et al* 1998). The resultant k-space difference functions for all three MX_3 systems display an FSDP which implies a contribution to this feature from the M–X correlations. The observed decrease in the position of the FSDP with increasing cation size is consistent with an enhanced separation in r-space of the cation centred polyhedral units (Salmon 1994).

The measured $\Delta G_M(r)$ show that there is an asymmetric distribution of anions about cations in the liquid state and that there is a reduction in $\bar{n}_M^X$ on melting (see table 3) from nine for MCl_3 and MBr_3 which melt from the UCl_3-type structure (Morosin 1968) and from eight for MI_3 which melts from the $PuBr_3$-type structure (Forrester *et al* 1964). In molten MCl_3 there is no evidence for a dominant number of stable and essentially regular MCl_6^{3-} octahedra which may be inferred from previous x-ray diffraction total structure factor and Raman scattering measurements on molten $LaCl_3$ and $CeCl_3$ (Mochinaga *et al* 1991, 1993, Iwadate *et al* 1995). Instead, integration of the first peak in $\Delta G_M(r)$ to the first shoulder gives a coordination number $\bar{n}_M^{Cl} = 6.7(2)$ which is larger than six while the ratio of the Cl–Cl to M–Cl nearest-neighbour distances $r_{ClCl}/r_{MCl} = 1.22(2)$ which is significantly smaller than the ratio of $\sqrt{2}$ expected for perfect octahedra. Interaction models based on the existence of rather stable MCl_6^{3-} octahedra are not therefore expected to quantitatively reproduce the structure and dynamics of molten $LaCl_3$ and $CeCl_3$ (Erbölükbas *et al* 1992). Notwithstanding, such models give $\bar{n}_M^{Cl} \approx 7$ and $r_{ClCl}/r_{MCl} \approx 1.25$, in good agreement with the present experiment, although $\bar{n}_{Cl}^{Cl}$ is too small at ≈5.4 (Tatlipinar *et al* 1992, 1993). The measured $\Delta G'(r)$ show that there is a reduction in $\bar{n}_X^X$ on melting (see table 3) from 12 for MCl_3 and MBr_3 which melt from the UCl_3-type structure (Morosin 1968) and from 11.3 for MI_3 which melts from the $PuBr_3$-type structure (Forrester *et al* 1964).

Table 3. Summary of the parameters obtained from the difference functions $\Delta G_M(r)$ and $\Delta G'(r)$ for molten LaX_3 and CeX_3 salts where $r_{\alpha\beta}$ denotes a mean nearest-neighbour distance.

Salt	r_{MX} (Å)	$\bar{n}_M^X$ [a]	$\bar{n}_M^X$ [b]	r_{XX} (Å)	$\bar{n}_X^X$ if $\bar{n}_M^M = 0$	$\bar{n}_X^X$ if $\bar{n}_M^M = 2$	r_{XX}/r_{MX}
MCl_3	2.93(2)	6.7(2)	8.2(2)	3.58(3)	10.3(2)	9.2(2)	1.22(2)
MBr_3	3.01(2)	6.1(2)	7.4(2)	3.76(3)	9.3(2)	8.7(2)	1.25(2)
MI_3	3.18(2)	5.1(2)	6.7(2)	4.13(2)	9.1(2)	8.2(2)	1.30(2)

[a] Integrating to the first shoulder in $\Delta G_M(r)$.
[b] Integrating to the first minimum in $\Delta G_M(r)$.

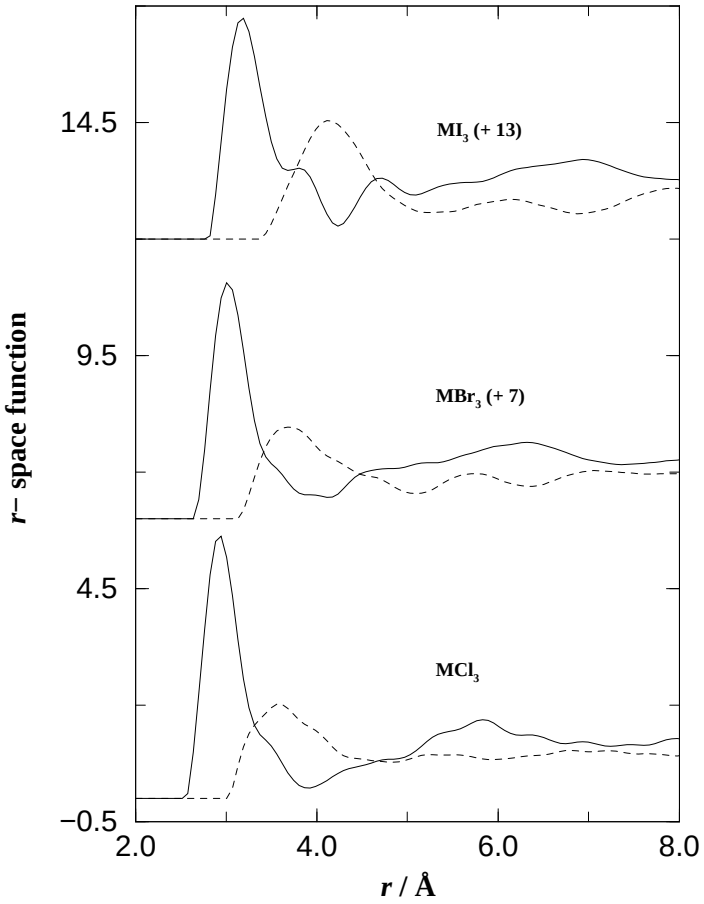

Figure 8. The real-space functions $[\Delta G_M(r) - \Delta G_M(0)]/2c_M c_X(b_{La} - b_{Ce})b_X$ (solid curves) and $[\Delta G'(r) - \Delta G'(0)]/c_X^2 b_X^2$ (broken curves), defined by equations (15) and (16) respectively, for the MCl_3, MBr_3 and MI_3 molten salts.

Since the first peaks in $\Delta G_M(r)$ and $\Delta G'(r)$ are identified with the M–X and X–X correlations respectively, it is instructive to compare the functions

$$[\Delta G_M(r) - \Delta G_M(0)]/2c_M c_X(b_{La} - b_{Ce})b_X = g_{MX}(r) + A' g_{MM}(r) \qquad (15)$$

and

$$[\Delta G'(r) - \Delta G'(0)]/c_X^2 b_X^2 = g_{XX}(r) - B' g_{MM}(r) \qquad (16)$$

where A' and B' are 0.228(5) and 0.0483(4) for MCl_3, 0.320(6) and 0.0958(9) for MBr_3, 0.415(9) and 0.159(2) for MI_3. The functions, plotted in figure 8, show a significant penetration of $g_{XX}(r)$ into the first peak of $g_{MX}(r)$ for all three molten salts which does not change markedly with increasing anion size. However, as shown in table 3 the increase in anion size promotes a decrease in both the $\bar{n}_M^X$ and $\bar{n}_X^X$ coordination numbers. The penetration of $g_{XX}(r)$ into the first peak of $g_{MX}(r)$ decreases with cation size for the molten trivalent metal halides (Saboungi *et al* 1993, Badyal *et al* 1994, Price *et al* 1998), a similar trend being observed for the molten divalent metal halides (Enderby and Biggin 1983, Wilson and Madden 1993).

6. Conclusions

In summary, the difference functions obtained by using the method of isomorphic substitution in neutron diffraction show that the FSDPs in the total structure factors have a strong contribution from the cation correlations and that on melting the MX_3 salts exhibit a reduction in both the $\bar{n}_M^X$ and $\bar{n}_X^X$ coordination numbers. In the molten state the M–X coordination environment is asymmetric and there is a significant penetration of $g_{XX}(r)$ into the first peak of $g_{MX}(r)$ for all three anions. This overlap does not change markedly with increasing anion size although there is a reduction in both the $\bar{n}_M^X$ and $\bar{n}_X^X$ coordination numbers.

Acknowledgments

It is a pleasure to thank Paul Madden for his encouragement of the present work, Takeshi Usuki, Spencer Howells, Chris Benmore, John Dreyer and Duncan Francis for help with the neutron diffraction experiments, Stephen Lovesey for useful correspondence on paramagnetic neutron scattering, Francis Hutchinson and Moises Silbert for useful discussions on MX_3 systems, Chris Anson for help with the crystal structures and the EPSRC for support.

References

Akdeniz Z and Tosi M P 1992 *Proc. R. Soc.* A **437** 85
Asprey L B, Keenan T K and Kruse F H 1964 *Inorg. Chem.* **3** 1137
Badyal Y S, Allen D A and Howe R A 1994 *J. Phys.: Condens. Matter* **6** 10 193
Balcar E and Lovesey S W 1989 *Theory of Magnetic Neutron and Photon Scattering* (Oxford: Clarendon)
Bleaney B I and Bleaney B 1989 *Electricity and Magnetism* 3rd edn, vol 2 (Oxford: Oxford University Press)
Brown P J 1995 *International Tables for Crystallography* vol C, ed A J C Wilson (Dordrecht: Kluwer) p 391
Cotton F A and Wilkinson G 1988 *Advanced Inorganic Chemistry* 5th edn (New York: Wiley)
Dworkin A S and Bredig M A 1971 *High Temp. Sci.* **3** 81
Enderby J E and Biggin S 1983 *Advances in Molten Salt Chemistry* vol 5, ed G Mamantov (Amsterdam: Elsevier) p 1
Erbölükbas A, Akdeniz Z and Tosi M P 1992 *Nuovo Cimento* D **14** 87
Forrester J D, Zalkin A, Templeton D H and Wallmann J C 1964 *Inorg. Chem.* **3** 185
Freeman A J and Desclaux J P 1979 *J. Magn. Magn. Mater.* **12** 11
Fukushima K and Iwadate Y 1996 *J. Alloys Compounds* **237** 6
Fukushima K, Iwadate Y, Andou Y, Kawashima T and Mochinaga J 1991 *Z. Naturf.* a **46** 1055
Gaune P, Gaune-Escard M, Rycerz L and Bogacz A 1996 *J. Alloys Compounds* **235** 143
Gaune-Escard M, Rycerz L, Szczepaniak W and Bogacz A 1994 *J. Alloys Compounds* **204** 193
Howe M A, McGreevy R L and Howells W S 1989 *J. Phys.: Condens. Matter* **1** 3433
Igarashi K and Mochinaga J 1987 *Z. Naturf.* a **42** 777
Iwadate Y, Okako N, Koyama Y, Kubo H and Fukushima K 1995 *J. Mol. Liq.* **65/66** 369
Janz G J, Dampier F W, Lakshminarayanan G R, Lorenz P K and Tomkins R P T 1968 *Natl Bur. Stand. Ref. Data Ser.* **15** 1
Janz G J, Tomkins R P T, Allen C B, Downey J R Jr, Gardner G L, Krebs U and Singer S K 1975 *J. Phys. Chem. Ref. Data* **4** 871
Janz G J, Tomkins R P T, Allen C B, Downey J R Jr and Singer S K 1977 *J. Phys. Chem. Ref. Data* **6** 409
Johnston D F 1966 *Proc. Phys. Soc.* **88** 37
Kojima T, Inoue T and Ishiyama T 1951 *J. Electrochem. Soc. Japan* **19** 383
Krämer K, Schleid T, Schulze M, Urland W and Meyer G 1989 *Z. Anorg. (Allg.) Chem.* **575** 61
Kutscher J and Schneider A 1974 *Z. Anorg. (Allg.) Chem.* **408** 121
Lond P B, Salmon P S and Champeney D C 1991 *J. Am. Chem. Soc.* **113** 6420
Madden P A and Wilson M 1996 *Chem. Soc. Rev.* **25** 339
Mellors G W and Senderoff S 1960 *J. Phys. Chem.* **64** 294
Mochinaga J, Ikeda M, Igarashi K, Fukushima K and Iwadate Y 1993 *J. Alloys Compounds* **193** 36
Mochinaga J, Iwadate Y and Fukushima K 1991 *Mater. Sci. Forum* **73–75** 147
Morosin B 1968 *J. Chem. Phys.* **49** 3007

Pettifor D G 1986 *J. Phys. C: Solid State Phys.* **19** 285
Price D L, Saboungi M-L, Badyal Y S, Wang J, Moss S C and Leheny R L 1998 *Phys. Rev.* B **57** 10 496
Saboungi M-L, Howe M A and Price D L 1990 *Proc. 7th Int. Symp. on Molten Salts* vol 90-17, ed C L Hussey *et al* (Pennington, NJ: Electrochemical Society) p 8
——1993 *Mol. Phys.* **79** 847
Salmon P S 1992 *Proc. R. Soc.* A **437** 591
——1994 *Proc. R. Soc.* A **445** 351
Salmon P S and Benmore C J 1992 *Recent Developments in the Physics of Fluids* ed W S Howells and A K Soper (Bristol: Hilger) p F225
Salmon P S, Xin S and Fischer H E 1998 *Phys. Rev.* B **58** 6115
Sears V F 1992 *Neutron News* **3** 26
Shannon R D 1976 *Acta Crystallogr.* A **32** 751
Soper A K, Howells W S and Hannon A C 1989 *Rutherford Appleton Laboratory Report* RAL-89-046
Squires G L 1978 *Introduction to the Theory of Thermal Neutron Scattering* (Cambridge: Cambridge University Press)
Tallon J L and Robinson W H 1982 *Phys. Lett.* A **87** 365
Tatlipinar H, Akdeniz Z, Pastore G and Tosi M P 1992 *J. Phys.: Condens. Matter* **4** 8933
——1993 *J. Phys.: Condens. Matter* **5** 991
Templeton D H and Dauben C H 1954 *J. Am. Chem. Soc.* **76** 5237
van der Aart S A, Verkerk P, Barnes A C, Salmon P S, Winter R, Fischer H, de Graaf L A and van der Lugt W 1998 *Physica* B **241–243** 961
Wasse J C 1998 *PhD Thesis* University of East Anglia, UK
Wasse J C and Salmon P S 1998 *Physica* B **241–243** 967
Wells A F 1984 *Structural Inorganic Chemistry* 5th edn (Oxford: Clarendon)
Wilson M and Madden P A 1993 *J. Phys.: Condens. Matter* **5** 6833
Yaffe I S and van Artsdalen E R 1956 *Chem. Semi Annu. Prog. Rep. Oak Ridge Natl Lab.* **2159** 77
Zachariasen W H 1948 *Acta Crystallogr.* **1** 265